



UNIVERSITÀ
DEGLI STUDI
DI UDINE

Università degli studi di Udine

Urban air pollution by odor sources: Short time prediction

Original

Availability:

This version is available <http://hdl.handle.net/11390/1067525> since 2020-02-25T10:28:34Z

Publisher:

Published

DOI:10.1016/j.atmosenv.2015.09.037

Terms of use:

The institutional repository of the University of Udine (<http://air.uniud.it>) is provided by ARIC services. The aim is to enable open access to all the world.

Publisher copyright

(Article begins on next page)

Urban air pollution by odor sources: short time prediction

Nicola Pettarin^{b,c}, Marina Campolo¹ and^a, Alfredo Soldati^{b,c}

^a*Dept. Chemistry, Physics & Environment,
University of Udine, 33100 Udine, Italy*

^b*Dept. Management, Electric & Mechanical Engineering,
University of Udine, 33100 Udine, Italy*

^c*LOD srl, 33100 Udine, Italy*

Abstract

A numerical approach is proposed to predict the short time dispersion of odors in the urban environment. The model is based on (i) a three dimensional computational domain describing the urban topography at fine spatial scale (one meter) and on (ii) highly time resolved (one minute frequency) meteorological data used as inflow conditions. The time dependent, three dimensional wind velocity field is reconstructed in the Eulerian framework using a fast response finite volume solver of Navier-Stokes equations. Odor dispersion is calculated using a Lagrangian approach. An application of the model to the historic city of Verona (Italy) is presented. Results confirm that this type of odor dispersion simulations can be used (i) to assess the impact of odor emissions in urban areas and (ii) to evaluate the potential mitigation produced by odor abatement systems.

Keywords: Dispersion modelling, short averaging time, odor pollution,

¹Corresponding author. Address via Cotonificio 108, 33100 Udine (UD), Italy; e-mail marina.campolo@uniud.it; phone: +39 432 558822; faxes: +39 432 558803

1. Introduction

Exposure to unpleasant odors is one of the most frequent causes of air quality complaints in both industrial and urban areas. The chemical compounds responsible for odor generation are volatile species (Olafsdottir and Gardarsson, 2013): once emitted from a source, their transport, dispersion and fate in the environment is controlled by the complex interaction among strength of emission (Campolo et al., 2005), meteorological conditions and site topography. Odors become perceptible whenever the instantaneous and local concentration of these chemicals transpasses very low concentration values corresponding to the odor detection threshold. This may occur nearby a source but also some distance away from it.

Odor perception is synchronous with breathing and involuntary, but the subsequent reaction to a given odor stimulus is to some degree subjective: it depends on odor intensity and offensiveness, duration and frequency of exposure but also on pleasantness/unpleasantness of the sensation evoked by the odor (Blanes-Vidal et al., 2012). Annoyance may be produced from acute exposure to few, high odor intensity events or to chronic exposure to repeated, low odor intensity events (Griffiths, 2014). Whichever the exposure mode, odors generating a negative appraisal induce changes in people behavior and may trigger a stress-mediated response which may develop into a public health concern. Bad smells which occasionally cause annoyance, are proactively reported to the Health Services: when the source of the odor can be clearly identified and associated to a specific emission either by the

24 analysis of resident nuisance odor reports (Nicolas et al., 2011), by the use
25 of chemical sensors (Sohn et al., 2009; Seo et al., 2011) or by other sensory
26 methods (Brattoli et al., 2011, Capelli et al., 2011), corrective actions can be
27 devised as needed to contain/reduce the odor impact.

28 Odor impact in urban areas can be very difficult to assess and control
29 due to the inherent complexity of the urban environment, the large num-
30 ber of potential sources and the local small scale variability of the dispers-
31 ing wind. Odor nuisance is most frequently associated with discontinuous
32 emissions generated by restaurants, fast food and bar which may occur for
33 short/prolonged times (from a few seconds to minutes), occasionally or on
34 a repetitive basis depending on the actual operating hours of the facility.
35 The odor impact potentially arising from these commercial activities should
36 be taken into account when planning new installations: best practices for
37 design and operation of commercial kitchen ventilation systems have been
38 developed (see DEFRA, 2005) and yet more accurate modelling tools could
39 be profitably used for odour pollution assessment, prevention and mitiga-
40 tion. Odor emissions in a high populated urban area could be confidently
41 authorized if the potential impact of each source could be estimated *a priori*
42 by modelling; moreover, the precise evaluation of the odour impact of an ex-
43 isting source might be required for the detailed analysis of resident nuisance
44 odor reports in support of litigations for odor impact problems.

45 Odor impact assessment based on chemical sensors would require the ac-
46 quisition of highly time resolved, compound specific, qualified low-concentration
47 data which are very difficult to obtain experimentally. Furthermore, most
48 odors are generated by mixtures of compounds and the relationship between

49 species concentration and odor nuisance is not straightforward. A more prac-
50 tical and effective approach may be the numerical prediction of odor disper-
51 sion.

52 Numerical models have been successfully used to predict odor dispersion
53 and to assess odor impact in industrial areas (see Nicell, 2009, Sironi et al.,
54 2010). The common approach is to model the odor as a passive chemical,
55 equivalent to the mixture of chemicals present, whose concentration is con-
56 veniently represented by the number of odor units, a multiple of the mixture
57 detection threshold. Most of the models in use has been adapted from ear-
58 lier studies on air pollution: steady state Gaussian plume models (Latos et
59 al., 2011), fluctuating plume models (Mussio et al., 2001; Dourado et al.,
60 2014) and Lagrangian stochastic dispersion models (Franzese, 2003) have
61 been used. The main challenge when using these models to predict odor
62 dispersion is related with the different time and space resolution at which
63 the prediction is required. The time scale of few seconds (corresponding to a
64 single human breath) required to evaluate odor impact is much smaller than
65 the hourly time scale typically used to evaluate the dispersion of pollutant
66 species. If a hourly time scale is maintained for odor dispersion modelling,
67 the peak odor concentration at the time scale relevant for odor impact as-
68 sessment should be estimated using a peak to mean ratio, which can be
69 either assumed to be constant (Sironi et al., 2010) or calculated based on
70 wind speed, atmospheric stability, distance from and geometry of the source
71 (Piringer et al., 2012; Schauburger et al., 2012).

72 Very different regulation limits and guidelines have been used worldwide
73 to fix benchmark concentration for odors: Nicell (2009) reports values of off-

74 site odor limits ranging from 0.5 to 50 odor units, averaging time ranging
75 from 1 s to 1 hr and compliance frequency ranging from 98% to 100%. In
76 Australia odor criteria (based on 3 minute average and 99.9% frequency) are
77 population density dependent (see EPA 373/07). The large variability in
78 odor exposure criteria indicates that there is still little consensus on what
79 odor concentration and/or averaging time represent the most effective and
80 fair odor limits for off-site impact. Recently, odor criteria have been clas-
81 sified into two groups (Sommer-Quabach et al., 2014): those based on low
82 odor concentration threshold and high exceedance frequency, relevant to as-
83 sess chronic exposure, and those based on high concentration threshold and
84 low exceedance frequency, relevant to assess acute exposure. At now, the rec-
85 ommended approach for odor regulation in Europe belongs to the first type
86 (chronic exposure oriented) and consists in predicting by numerical models
87 the hourly mean of odor concentration for at least one year period (up to 3 or
88 5 years) and to check odor exposure considering the 98th percentile of those
89 data (see Environment Agency, 2011). The choice of the 98th percentile
90 is supported by the strong correlation found with annoyance measured by
91 community surveys (see Pullen and Vawda, 2007). Yet, different assessment
92 tools and regulatory responses may be required to effectively manage acute
93 exposure scenario (Griffiths, 2014).

94 A possibility is to use a smaller time scale for the odor dispersion mod-
95 elling by which the peaks in odor concentration which result in annoyance
96 for the population can be directly captured: Drew et al. (2007) demon-
97 strated that dispersion modelling based on short averaging time was more
98 successful than the current regulatory method at capturing odor peak con-

centrations from a landfill site. Peak odor intensity is often associated with relatively weak meteorological dynamics (light winds) for which short term and short range effects may be important: wind directions can be highly variable (Huiling-cui et al., 2011), turbulent motions may be of the same order as wind speed and the shear production term may dominate in the turbulent kinetic energy budget equation (Manor, 2014) making the turbulent transport of species more sensitive to the presence of boundaries (complex terrain and presence of buildings) and highly anisotropic (Pitton et al., 2012).

Eulerian-Eulerian models based on Reynolds Averaged Navier Stokes (RANS) equations and Large Eddy Simulation (LES) have proven to be accurate to simulate the dispersion of chemical species (pollutants) in complex three dimensional domains (Hanna et al., 2006). Gailis et al. (2007) investigated tracer dispersion in a boundary layer sheared by a large array of obstacles using a Lagrangian stochastic plume model. They found that internal plume fluctuations can have a greater effect on tracer dispersion than the meander motion of the plume, which may be significantly damped in a rough-walled boundary layer. Michioka et al. (2013) implemented a short term, highly resolved (10 s) microscale large-eddy simulation (LES) model coupled to a mesoscale LES model to estimate the concentration of a tracer gas in an urban district considering both the influence of meteorological variability and topographic effects. Their results underlined the key role of coupling between mesoscale and local atmospheric dynamics in driving the dispersion of tracer gas.

The same type of short term, fine scale models can be used to simulate odor dispersion in the urban environment. Odor dispersion under steady

124 wind and constant emission in the presence of few buildings has been eval-
 125 uated using Eulerian-Eulerian Re-Normalisation Group (RNG) $k - \epsilon$ model
 126 by Maizi et al. (2010), using Large Eddy Simulation (LES) by Dourado et
 127 al. (2012) and using a fluctuating plume model by Dourado et al. (2014).
 128 Despite the increasing number of applications based on local, short averaging
 129 time dispersion models, this modelling approach has not yet been adequately
 130 validated to be confidently used for odor impact assessment (Pullen and
 131 Vawda, 2007). Moreover, we are not aware of applications of odor dispersion
 132 models to more complex urban environments. One of the reason is most likely
 133 the high cost associated with the time-dependent, fine resolved calculations
 134 needed to characterize the flow field of the carrier fluid and the transport of
 135 dispersed species into a complex domain. A fine spatial grid resolution (order
 136 of 1-2 meters) is required to model faithfully the complex urban domain and
 137 a fine time resolution is required to model concentration fluctuations and to
 138 capture the peak values responsible of the impact (see Pullen and Vawda,
 139 2007). The simulation of local atmospheric dynamics highly resolved in space
 140 and time may become cheaper if representative scenarios rather than full year
 141 periods can be identified and considered. Moreover, cost/time of computa-
 142 tion can be reduced adopting fast response models of Eulerian-Lagrangian
 143 type developed and used successfully to calculate dispersion of species in
 144 urban environments (Gowardhan et al., 2011).

145 In this work we propose the use of one of these models (QUIC – Quic
 146 Urban & Industrial Complex model, Los Alamos Laboratories) (Gowardhan
 147 et al., 2011) to evaluate the impact of odor emissions in urban environments.
 148 The work is based on the assumption that the local wind field and turbulence

149 controlling dispersion is triggered by the urban geometry more than by the
150 microscale wind and atmospheric turbulence. Our objective is to demonstrate
151 how different can be the odor impact evaluated in the short term when the
152 dynamic interaction between wind field and complex urban topography is
153 accounted for. We will use highly resolved (one minute frequency) microscale
154 wind velocity data to reconstruct the flow field around buildings; this flow
155 field will then be used to simulate the transport of odor, to evaluate odor
156 exposure in terms of frequency of exceedance and intensity and to assess the
157 potential odor impact. To demonstrate our idea, two different meteorological
158 scenarios will be considered. Increasing the number of simulated scenarios
159 enough to cover all the meteorological conditions that may influence the
160 impact, the model could become a powerful tool to help Public Authorities
161 in their planning and control activities.

162 First, we will to demonstrate that the proposed model can be used to
163 evaluate comparatively the odor impact of a given emission source when
164 located in alternative positions inside the urban micro-environment; second,
165 we will prove that the model can be used to check if the odor impact can be
166 sufficiently abated by the installation of odor control systems. The potential
167 of the model will be demonstrated comparing the effect of untreated/treated
168 emission associated to the planned installation of fast food activities in two
169 different urban zones in the historical city of Verona (Italy).

170 **2. Methods, site and data**

171 *2.1. Numerical model*

172 The model proposed (QUIC) is a 3D finite volume solver of Reynolds-
173 Averaged Navier-Stokes (RANS) equations for incompressible flow. The
174 model is implemented and runs in the Matlab environment. The compu-
175 tational domain, corresponding to an urban area including a large number
176 of buildings, is defined using a structured grid in which solid/fluid cells are
177 identified using numerical coding (zero and one identify solid and fluid cells,
178 respectively). The grid is generated from Environmental Systems Research
179 Institute (ESRI) shape files using the code built-in pre-processor.

180 RANS equations are solved explicitly in time on a staggered mesh using
181 a projection method. The discretization scheme is second order accurate
182 in space and time (see Gowardhan et al., 2011 for further details). A zero
183 equation (algebraic) turbulence model is used. Free slip conditions are used
184 at the top and side boundaries of the computational domain; a prescribed,
185 time dependent velocity profile derived from an urban meteorological station
186 can be imposed at the upwind side while an outflow boundary condition is
187 imposed at the downwind side.

188 A Lagrangian particle approach is used to model odor dispersion: thou-
189 sands of "particles" released from the emission point are tracked as they
190 are randomly advected and dispersed over the domain (Zwack et al., 2011).
191 Particles are modeled as infinitesimally small, neutrally buoyant gas parcels.
192 For the present application, a steady state emission is considered for the odor
193 plume: each particle is associated with a fraction of the odor emission rate
194 and is tracked using a small time step (0.1 seconds). Overall, about half

195 a million QUIC particles were released over the simulation time period (15
196 minutes).

197 Odor concentrations are determined in the Eulerian reference frame by
198 counting how many particles pass through a given computational volume
199 during the time averaging period of interest (30 seconds in our demo).

200 2.2. Urban district

201 Figure 1 (a) shows an aerial view of Verona downtown (near to the Arena).
202 Two different zones were selected for modelling odor dispersion to check
203 whether the specific localization of the source could significantly affect odor
204 impact: the first area (230×290 m wide), identified as Area 1, is characterized
205 by street canyons; the second area (495×250 m wide), identified as Area
206 2, faces the open square of the Arena. Figures 1 (b) and (c) show the two
207 computational models which extend 50 m above the ground.

208 The potential positions of the odor emission source in Area 1 and Area
209 2 are shown as red (light gray) dots $S1$ and $S2$. The emission height was
210 fixed as one meter above the roof level. In the local coordinates system,
211 with the grid origin at the lower left corner of each area, source positions
212 are identified by (x, y, z) triples equal to $(138.5, 176.5, 18.5)$ for Area 1 and
213 $(161.5, 238.5, 17.5)$ for Area 2. The blue (dark gray) circles indicate control
214 points P_1 and P_2 located 50 m downstream the source in the prevailing wind
215 blowing direction. The elevation of control points is 1.5 m above the ground.

216 2.3. Meteorological data

217 Data used in this work are taken from the urban station of Verona Golo-
218 sine (latitude $45^\circ 28' 51''$, longitude $10^\circ 52' 35''$, 61 m above sea level). One-

219 minute time resolved records of wind speed and direction collected during
 220 February 2012 were made available from MeteoVerona. One week of data was
 221 statistically analysed. Statistics suggest that the prevailing wind blowing di-
 222 rection is from **Nord**, North-East (N-E) and the average wind speed is about
 223 0.89 m/s at the wind monitoring station (10 m elevation above the ground).
 224 To demonstrate how different can be the odor impact evaluated in the short
 225 term when time dependent winds interact with a complex urban topography,
 226 two 15 minute long periods were extracted for modelling odor dispersion: the
 227 first, event 1, is characterized by wind intensity of $3.12 \pm 0.67\text{ m/s}$ (average
 228 plus standard deviation) and wind blowing from direction $48 \pm 44^\circ$ degrees
 229 N (average plus standard deviation); the second, event 2, is characterized
 230 by wind intensity of $3.3 \pm 1.2\text{ m/s}$ and wind blowing from direction $2 \pm 20^\circ$
 231 degrees N. Even if average wind intensity is similar, variability of wind in-
 232 tensity is larger for event 2, whereas wind directions differ both in average
 233 value and variability. The two events selected are examples of “similar” and
 234 yet substantially different scenarios which need to be simulated to obtain
 235 a consistent evaluation of odor impact. Considering the size of computa-
 236 tional domain and average wind intensity, each 15 minute long period is long
 237 enough to track the dispersion of the odor plume up to the boundaries of the
 238 computational domain. More/longer periods could be routinely simulated
 239 once extended meteorological data are made available.

240 Figure 2 shows the wind variation of the two selected events using a
 241 polar representation (Figure 2 (a)) and time series plots of wind speed and
 242 direction (Figure 2 (b) and (c)). At each time step, the direction from which
 243 the wind is blowing identifies the upstream side of the computational domain;

the vertical profile of wind velocity used as inflow condition is defined by the wind speed recording at the anemometer (red arrow in Figure 1 (b)) using a power law.

2.4. Emission data

To characterize the strength of the emission, we considered a restaurant using the same cooking methods (deep frying and stewing) of the planned fast food installation. Samples used to quantify the odor emission rate were collected from the chimney of the restaurant when a frying food system was active. The mean cooking time for lunch (or dinner) period was 109 minutes. The stack diameter was 1 m. The mean values of stack outlet velocity and exhaust flow rate were 4.12 m/s and 350 Nm^3/min . The mean stack inlet and outlet temperatures were 44°C and 31°C. The variability of the source was checked during sampling according to EN ISO 16911:2013. We collected three samples according to EN 13725:2003 using a vacuum pump to suck air from the emitting stack into Nalophan bags (8 L volume); sampling required about 1.5 minutes for each sample, with 10 minute stop between samples to check emission variability over time; odor samples were then transferred to the lab for the sensory evaluation of odors off site by a group of trained panels. Mixtures of sampled air and neutral air at decreasing dilution ratio were sequentially prepared by the olfactometer and smelt by the panels. The test started from an odor sample which was very diluted. The dilution ratio was gradually reduced up to the identification of the odor threshold, i.e. the point at which the odor is only just detectable to 50% of the test panel. The numerical value of the dilution ratio necessary to reach the odor threshold was taken as the measure of the odor concentration at the source expressed

269 in European odor units per cubic meter ($o.u._E/m^3$, ou/m^3 in brief).

270 Sampling was performed in two different working conditions, correspond-
271 ing to off/on operation for the activated carbon filter installed for odor con-
272 trol. Data collected during sampling are summarized in Table 1. Data vari-
273 ability during sampling and among samples was found to be not significant
274 and odor emission rates used to set up the model are values averaged over
275 the three samples.

276 3. Results

277 3.1. Flow field

278 The QUIC code calculates the flow field in the three dimensional do-
279 main every one minute. Figure 3 shows the comparison between the wind
280 speed/direction measured at the meteorological station (10 m height, line
281 with circles) and used as inflow condition, and those calculated in differ-
282 ent points of the computational domain: at the source (1 m above roof level,
283 empty triangles) and at the reference control point (solid triangles) for Area 1
284 (triangles pointing upward) and Area 2 (triangles pointing downward) (1.5 m
285 above ground). The effect of urban topography is to produce local differences
286 in wind intensity and direction calculated at different points.

287 Wind speed and direction calculated at the emission point (i.e. above
288 the buildings) are similar to the values recorded at the meteorological sta-
289 tion: the wind speed is a bit larger at the emission point since it is more
290 elevated than the anemometric sensor. At control points, the wind speed
291 is generally smaller than the sensor due to the different elevation above the
292 ground (1.5 m); the wind direction may be significantly different. For control

293 points located in a street canyon, the effect of the urban topography is to
 294 smooth out the variability of wind direction. For wind event 1, the local wind
 295 direction is about $50^\circ N$ whichever the value recorded at the meteorological
 296 station for both control points P1 and P2; for event 2, the wind direction
 297 is similar at the meteorological station and point P2, whereas it is always
 298 about $50^\circ N$ for point P1.

299 3.2. Odor dispersion

300 Animations of the odor plume dispersing from sources S1 and S2 during
 301 the two simulated wind events are available as supplementary material. The
 302 position of the emission point is indicated by the black circle; isocontours
 303 represent the odor concentration (in ou/m^3) calculated in the plane 1.5 m
 304 above the ground (reference height of human noses potentially smelling in
 305 the area). Figures 4-5 shows snapshots (one every 240 seconds) taken from
 306 the animations. The color scale for odor concentration shown in the plots
 307 is limited to the sub-range $[2 \div 12\ ou/m^3]$. To relate odor concentration to
 308 perceived odor intensity in the field we refer to the following scale (Sommer-
 309 Quabach et al., 2014): non detectable ($C < 2\ ou/m^3$), acceptable ($2 <$
 310 $C < 5\ ou/m^3$), annoyance ($5 < C < 15\ ou/m^3$) and severe annoyance
 311 ($C > 15\ ou/m^3$). The lower and upper values of the color scale represent
 312 an odor concentration threshold at which the odor is clearly detected and a
 313 value at which the odor perceived is strong enough to cause annoyance.

314 Isocontours calculated during wind event 1 in Area 1 (Figure 4 upper
 315 row) show the odor plume extending in different directions depending on
 316 the leading wind. Yet, the urban topography determines a preferential path
 317 for odor dispersion which spreads along the main street canyons near to the

318 source. Due to the changing wind direction, some of the odor puffs may reach
 319 regions not directly exposed to the emitting source, producing diffuse odor
 320 impact even at significant distances. During wind event 2, isocontours (Fig-
 321 ure 4 bottom row) show odor puffs moving along three main street canyons
 322 (aligned with the wind blowing directions) with odor concentration mainly
 323 controlled by wind speed. Odor dispersion produced in Area 2 (open area
 324 facing the Arena) for wind event 1 (Figure 5 top row) indicates that odor
 325 puffs remain confined along the prevailing wind direction (from N-E to S-
 326 W) despite the wind direction variability, and may penetrate into the urban
 327 topography when the blowing wind direction is from S-E. For wind event 2
 328 (Figure 5 bottom row) the odor plume oscillates back and forth in the open
 329 square facing the Arena.

330 The dynamic evolution of odor isocontours gives a qualitative idea of
 331 the odor impact expected from the emission, given the position and the
 332 meteorological scenario. Yet, for a quantitative comparison we need more
 333 synthetic descriptors which can be obtained from the statistical analysis of
 334 the time series of odor concentration calculated for each grid point of the
 335 computational domain.

336 Figure 6 shows the time series of odor concentration calculated during
 337 wind event 1 for the grid point closest to the emission source S1 and for
 338 point P1. According to the FIDOL methodology (see Environment Agency,
 339 2011) the intensity and frequency of odor exposure are two of the main char-
 340 acteristics necessary to assess the offensiveness of odors. Due to the short
 341 averaging time and brief simulation period used in this work we can not use
 342 the recommended regulation approach to assess odor impact. We propose to

343 use two odor impact criteria similar to those discussed by Griffiths (2014),
 344 based on either intensity or frequency of odor impact events evaluated over
 345 the time interval of interest (the 15 minute long period in our case). Specif-
 346 ically, for the first odor criteria, we fix the frequency of exceedance (10%)
 347 and derive odor concentration isocontours which can be compared against
 348 threshold values; for the second odor criteria, we fix an odor concentration
 349 threshold ($C_{ref} = 5 \text{ ou}/m^3$) and derive maps of frequency of exceedance. Any
 350 specific value of frequency of exceedance and odor concentration threshold
 351 could be adopted to perform the kind of analysis we propose.

352 Figure 6 shows that near to the source (S1) the odor concentration is
 353 quite large ($653 \pm 100 \text{ ou}/m^3$ average value \pm standard deviation, coefficient
 354 of variation equal to 0.15) and only slightly changing over time; at point
 355 P1, the odor intensity is significantly lower ($11 \pm 8.7 \text{ ou}/m^3$ average value \pm
 356 standard deviation, coefficient of variation equal to 0.79) but the variability
 357 in time is larger. The 90th percentiles are equal to 24.4 (indicated as dashed
 358 thin line in the graph) and 802.6 ou/m^3 (not shown) for P1 and S1; the
 359 reference threshold concentration C_{ref} (dashed thick line in the graph) is
 360 exceeded 80% of time at P1 and 100% of time at S1.

361 Figure 7 shows the results of this analysis replicated for each point of
 362 the computational grid: this can be used to compare and rank, according
 363 to the two proposed assessment criteria, the odor impacts for Area 1 and
 364 Area 2 for simulated wind events. Isocontours of 90th percentile of odor
 365 concentration are shown in the top row and isocontours of the exceedance
 366 frequency ($C > C_{ref}$) are shown in the bottom row. These maps show
 367 the area in which any plotted concentration of odor is exceeded 10% of the

time at maximum, or the area in which detectable odor may be perceived persistently (i.e. most frequently) in time.

Comparison between isocontours of 90th percentile calculated for Area 1 and Area 2 for wind event 1 (Figure 7, left half) indicates that the emission will produce annoyance/severe annoyance at least 10% of the time along the main street canyon in Area 1 and in front of the buildings facing the Arena in Area 2. Detectable odor will be perceived for more than 50% of the time in these areas.

The odor impact becomes even more significant for wind event 2 (Figure 7, right half). In this case, the emission will produce annoyance/severe annoyance at least 10% of the time along the three street canyons for Area 1 and in a wide area close to the Arena in Area 2. Detectable odor will be perceived for more than 50% of the time in even wider areas.

Figure 8 shows a final synthetic picture of odor impact given in the form of odor roses, i.e. polar plots in which (i) the 90th percentile of odor concentration (top half) or (ii) the percent frequency of exceedance of C_{ref} (bottom half) are plotted at reference distances (5, 25 and 45 m away from the emission point) for each angular direction. Top and bottom rows in each half represent the impact of the emission as is (untreated) or when the odor abatement system is on. The radial scale of each plot is shown in the bottom right corner. Consider first the impact of untreated source, S1 and S2, for wind event 1 (first row, left half). The peak of odor concentration is found in the south-west (S-W) direction, with odor concentrations as large as 20 ou/m^3 25 and 45 m away from emission point S1 and as large as 40 ou/m^3 25 and 45 m away from emission point S2. Minor peaks are also found along those

393 directions in which the wind and the local topography are “in phase”. The
 394 frequency of exceedance of C_{ref} (third row, left half) is up to 60% both 25
 395 and 45 m away from emission point S1 in the S-W direction, and up to 55%
 396 and 75% respectively 25 and 45 m away from emission point S2 in the same
 397 direction. When the abatement system is on (second and fourth rows), the
 398 odor impact becomes lower than $10\text{ ou}/\text{m}^3$ whichever the distance and an-
 399 gular direction and C_{ref} is exceeded 50% of the time at most. The right half
 400 of Figure 8 shows the odor impact for wind event 2. In this case, the peak of
 401 odor concentration is in the south-south-west (S-S-W) direction, with odor
 402 concentrations as large as 40 and $76\text{ ou}/\text{m}^3$ respectively 5 m and 25 m away
 403 from emission point S2. The frequency of exceedance is about 100% 25 m
 404 and 45 m away from S2 in the S-W direction. These data indicate a more
 405 intense and persistent odor impact for wind event 2. The odor impact can
 406 be reduced in Area 1 treating the emission (second and fourth rows), with
 407 annoying odor perceived less than 40% of the time 25 m away from the source
 408 in the S-W direction. Annoying odor can be still perceived up to 60% of the
 409 time 45 m away from the source in the W-S-W direction. The situation is
 410 more critical for the source located in Area 2: even if the abatement system
 411 reduces the odor impact, annoying odor will still be perceived 80% of the
 412 time in the S-W direction 25 and 45 m away from the source.

413 4. Conclusions

414 In this work we propose the use of a fast response Eulerian-Lagrangian
 415 type model to calculate the short term, short time average dispersion of odor
 416 in urban areas. The model is based on a three dimensional computational

417 domain describing the urban topography at fine (one meter) spatial scale and
418 on highly time resolved (one minute frequency) meteorological data used as
419 inflow conditions.

420 We propose two odor impact criteria similar to those discussed by Griffiths
421 (2014) to assess odor impact: for the first odor criteria we fix the frequency
422 of exceedance (10%) to derive odor concentration isocontours which can be
423 compared against threshold values; for the second odor criteria we fix an
424 odor concentration threshold ($C_{ref} = 5 \text{ ou}/m^3$) to derive maps of frequency
425 of exceedance. Simulations performed for the historical city of Verona for
426 two 15 minute long time periods show that the model can be used (i) to
427 comparatively evaluate and rank the odor impact of a given emission source
428 when located in alternative positions of the urban area; (ii) to check if end of
429 pipe technologies devised for odor control are effective or not to reduce the
430 impact.

431 We propose the odor rose plot of model output statistics (90th percentile
432 and exceedance frequency) as a simple graphical tool to compare odor impact
433 for different source locations and in different meteorological scenarios and to
434 evaluate the effectiveness of solutions proposed for odor impact mitigation.

435 **Acknowledgements**

436 The authors would like to thank Comune di Verona for geographical data
437 and R. Snidar and S. Rivilli for fruitful discussions. M.C. gratefully acknowl-
438 edges Michael Brown and R&D staff of Los Alamos National Laboratory for
439 the use of QUIC code and technical support, and MeteoVerona for the acqui-
440 sition of highly resolved wind data. N.P. gratefully acknowledges Laboratorio

- 441 di Olfattometria Dinamica, Udine, Italy for funding his PhD fellowship.
- 442 [1] Blanes-Vidal, V., Suh, H., Nadimi, E.S., Løfstrøm, P., Ellermann, T.,
 443 Andersen, E.V., Schwartz, J., 2012, Residential exposure to outdoor
 444 air pollution from livestock operations and perceived annoyance among
 445 citizens, *Environment International*, 40: 44-50.
- 446 [2] Brattoli, M., de Gennaro, G., de Pinto, V., Loiotile, A.D., Lovascio, S.,
 447 Penza, M., 2011, Odour Detection Methods: Olfactometry and Chemical
 448 Sensors, *Sensors*, 11(5): 5290-5322.
- 449 [3] Campolo, M., Salvetti, M.V., Soldati, A., 2005, Mechanisms for mi-
 450 croparticle dispersion in a jet in crossflow, *AIChE J.*, 51(1): 28-43.
- 451 [4] Capelli, L., Sironi, S., Del Rosso, R., Centola, P., Rossi, A., Austeri, C.,
 452 2011, Olfactometric approach for the evaluation of citizens' exposure
 453 to industrial emissions in the city of Terni, Italy, *Science of the Total*
 454 *Environment*, 409: 595-603.
- 455 [5] DEFRA, Department for Environment, Food and Rural Affairs 2005,
 456 Guidance on the Control of Odour and Noise from Commercial Kitchen
 457 Exhaust Systems, Nobel House, 17 Smith Square, London SW1P 3JR.
- 458 [6] Dourado, H., Santos, J.M., Reis, N.C., Mavroidis, I., 2012, Numerical
 459 modelling of odour dispersion around a cubical obstacle using large eddy
 460 simulation, *Water Science and Technology*, 66(7): 1549-1557.
- 461 [7] Dourado, H., Santos, J.M., Reis, N.C., Mavroidis, I., 2014, Development
 462 of a fluctuating plume model for odour dispersion around buildings,
 463 *Atmospheric Environment*, 89: 148-157.

- 464 [8] Drew, G.H., Smith, R., Gerard, V., Burge, C., Lowe, M., Kinnersley, R.,
465 Sneath, R., Longhurst, P.J., 2007, Appropriateness of selecting different
466 averaging times for modelling chronic and acute exposure to environ-
467 mental odours, *Atmospheric Environment*, 41(13): 2870-2880.
- 468 [9] EN 13725:2003, Air quality – Determination of odour concentration by
469 dynamic olfactometry.
- 470 [10] EN ISO 16911:2013, Stationary source emissions – Manual and auto-
471 matic determination of velocity and volume flow rate in ducts – Part 1:
472 Manual reference method.
- 473 [11] Environment Agency, 2011, Additional guidance for H4 Odor Manage-
474 ment: How to comply with your environmental permit, Environment
475 Agency Horizon House, Deanery Road Bristol, BS1 5AH.
- 476 [12] EPA 373/07 guidelines: Odour assessment using odour source modelling,
477 2007, www.epa.sa.gov.au/files/477172_guide_odour.pdf
- 478 [13] Franzese, P., 2003, Lagrangian stochastic modeling of a fluctuating
479 plume in the convective boundary layer, *Atmospheric Environment*,
480 37(12): 1691-1701.
- 481 [14] Gailis, R.M., Hill, A., Yee, E., Hilderman, T., 2007, Extension of a
482 fluctuating plume model of tracer dispersion to a sheared boundary layer
483 and to a large array of obstacles, *Boundary-Layer Meteorol.*, 122: 577-
484 607.
- 485 [15] Gowardhan, A.A., Pardyjak, E. R., Senocak, I., Browm, M.J., 2011, A

486 CFD-based wind solver for an urban fast response transport and disper-
487 sion model, *Environmental Fluid Mechanics*, 11(5): 439-464.

488 [16] Griffiths, K.D., 2014, Disentangling the frequency and intensity dimen-
489 sions of nuisance odour, and implications for jurisdictional odour impact
490 criteria, *Atmospheric Environment*, 90: 125-132.

491 [17] Hanna, S.R., Brown, M.J., Camell, F.E.; Chan, S.T., Coirier, W.J.,
492 Hansen, O.R., Huber, A.H., Kim, S., Reynolds, R.M., 2006, Detailed
493 simulations of atmospheric flow and dispersion in downtown Manhattan:
494 An application of five computational fluid dynamics models, *Bulletin of*
495 *the American Meteorological Society*, 87(12): 1713-1726.

496 [18] Huiling cui, Yao, R., Xu, X., Xin, C., Yang, J., 2011, A tracer experiment
497 study to evaluate the CALPUFF real time application in a near-field
498 complex terrain setting, *Atmospheric Environment*, 45: 7525-7532.

499 [19] Latos, M., Karageorgos, P., Kalogerakis, N., Lazaridis, M., 2011, Disper-
500 sion of Odorous Gaseous Compounds Emitted from Wastewater Treat-
501 ment Plants, *Water Air Soil Pollut.*, 215: 667-677.

502 [20] Maizi, A., Dhaouadi, H., Bournot, P., Mhiri, H., 2010, CFD prediction of
503 odorous compound dispersion: Case study examining a full scale waste
504 water treatment plant, *Biosystems Engineering*, 106: 68-78.

505 [21] Manor, A., 2014, A Stochastic Single-Particle Lagrangian Model for
506 the Concentration Fluctuations in a Plume Dispersing Inside an Urban
507 Canopy, *Boundary-Layer Meteorology*, 150(2): 327-340.

- 508 [22] Michioka, T., Sato, A., Sada, K., 2013, Large-eddy simulation coupled to
509 mesoscale meteorological model for gas dispersion in an urban district,
510 Atmospheric Environment, 75: 153-162.
- 511 [23] Mussio, P., Gnyp, A.W., Hensha, P.F., 2001, A fluctuating plume dis-
512 persion model for the prediction of odour-impact frequencies from con-
513 tinuous stationary sources, Atmospheric Environment, 35: 2955-2962.
- 514 [24] Nicell, J.A., 2009, Assessment and regulation of odour impacts, Atmo-
515 spheric Environment, 43 (1): 196-206.
- 516 [25] Nicolas, J., Cors, M., Romain, A.C., Delva, J., 2011, Identification of
517 odour sources in an industrial park from resident diaries statistics, At-
518 mospheric Environment, 44(13): 1623-1631.
- 519 [26] Olafsdottir, S., Gardarsson, S.M., 2013, Impacts of meteorological fac-
520 tors on hydrogen sulfide concentration downwind of geothermal power
521 plants, Atmospheric Environment, 77: 185-192.
- 522 [27] Piringer, M., Schauburger, G., Petz, E., Knauder, W., 2012, Comparison
523 of two peak-to-mean approaches for use in odour dispersion models,
524 Water Science and Technology, 66(7): 1498-1501.
- 525 [28] Pitton, E., Marchioli, C., Lavezzo, V., Soldati, A., Toschi, F., 2012,
526 Anisotropy in pair dispersion of inertial particles in turbulent channel
527 flow, Phys. Fluids, 24(7): 073305.
- 528 [29] Pullen, J., Vawda, Y., 2007, Review of Dispersion Modelling for Odour
529 Predictions, Science Report: SC030170/SR3 Environment Agency, Rio
530 House, Waterside Drive, Aztec West, Almondsbury, Bristol, BS32 4UD

- 531 [30] Schaubberger, G., Piringer, M., Schmitzer, R., Kamp, M., Sowa, A.,
532 Koch, R., Eckhof, W., Grimm, E., Kypke, J., Hartung, E., 2012, Con-
533 cept to assess the human perception of odour by estimating short-time
534 peak concentrations from one-hour mean values. Reply to a comment
535 by Janicke et al., *Atmospheric Environment*, 54: 624-628.
- 536 [31] Sironi, S., Capelli, L., Centola, P., Del Rosso, R., Pierucci, S., 2010,
537 Odour impact assessment by means of dynamic olfactometry, dispersion
538 modelling and social participation, *Atmospheric Environment*, 44(3):
539 354-360.
- 540 [32] Sohn, J.H., Pioggia, G., Craig, I.P., Stuetz, R.M., Atzeni, M.G., 2009,
541 Identifying major contributing sources to odour annoyance using a non-
542 specific gas sensor array, *Biosystems Engineering*, 102(3): 305-312.
- 543 [33] Sommer-Quabach, E., Piringer, M., Petz, E., Schaubberger, G., 2014,
544 Comparability of separation distances between odour sources and resi-
545 dential areas determined by various national odour impact criteria, *At-*
546 *mospheric Environment*, 95: 20-28.
- 547 [34] Zwack, L.M., Hanna, S.R., Spengler, J.D., Levy, J.I., 2011, Using ad-
548 vanced dispersion models and mobile monitoring to characterize spatial
549 patterns of ultrafine particles in an urban area, *Atmospheric Environ-*
550 *ment*, 45(28): 4822-4829.

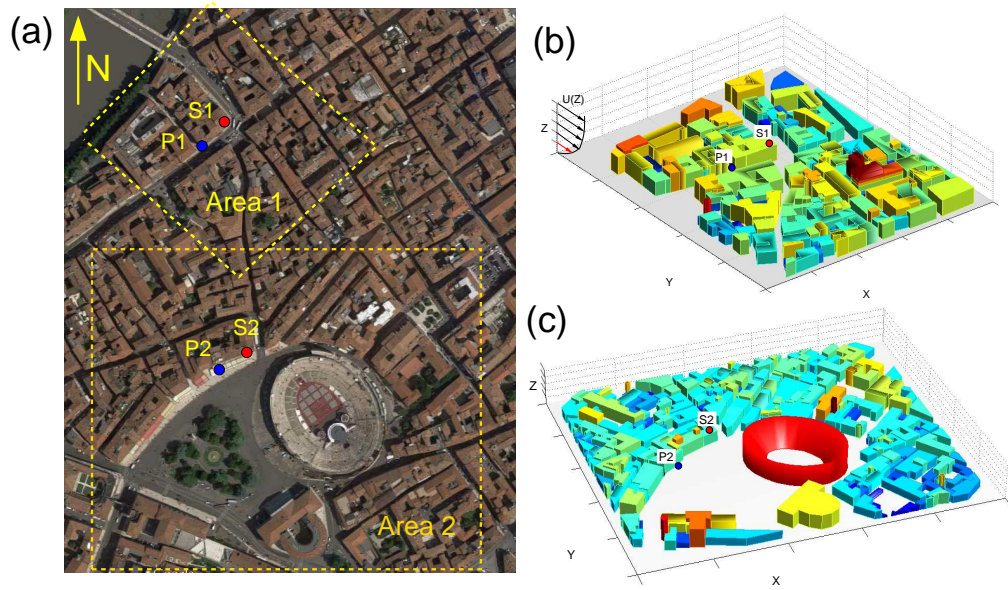


Figure 1: Aerial view of Verona (a) and areas selected for odor dispersion demo: (b) street canyons (Area 1) and (c) open square nearby the Arena (Area 2); potential positions of odor emission source are shown as (light gray) red circles (S1 and S2); points 50 m away from the source downstream the prevailing blowing wind direction (N-E) are shown as (dark gray) blue circles (P1 and P2).

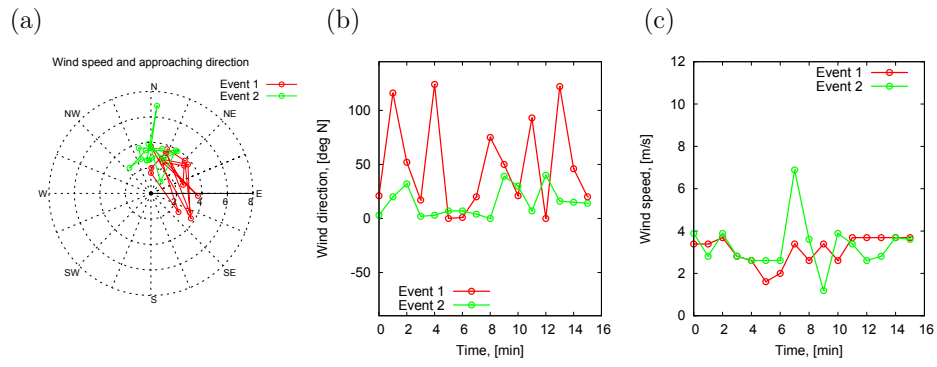


Figure 2: Polar representation (a) and time series plots of wind direction (b) and wind speed (c) of wind data extracted for simulating odor dispersion: data are taken from meteorological station of Verona Golosine.

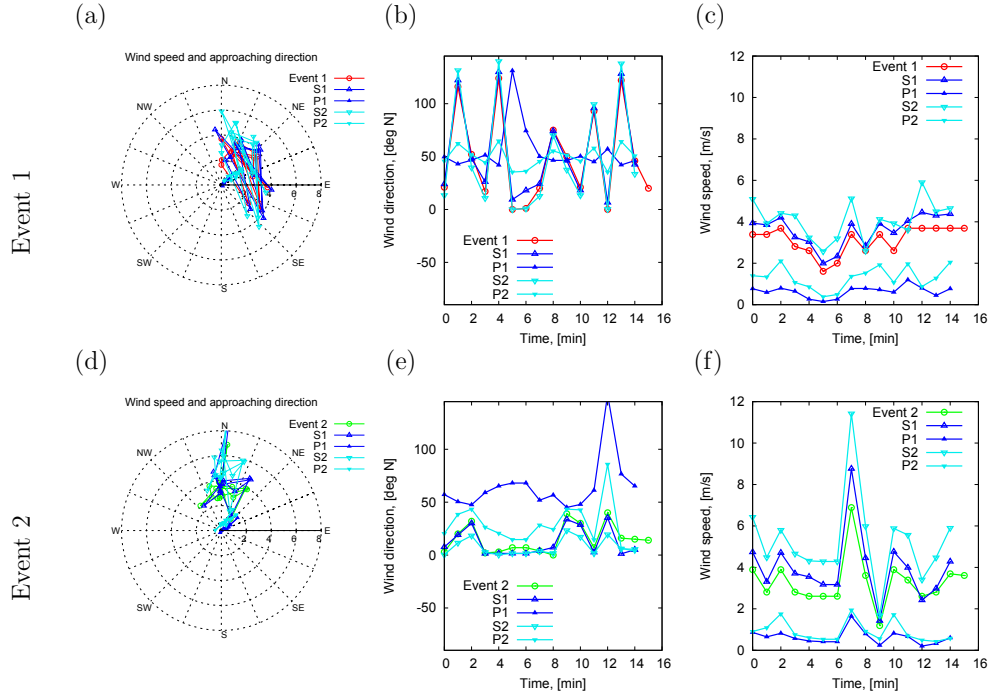


Figure 3: Polar representation (a, d) and time series plots of wind direction (b, e) and wind speed (c, f) calculated in different points of the computational domain for wind events 1 (top row) and 2 (bottom row): lines with symbols correspond to (i) anemometric data used as inflow condition (10 m above ground) (red/green, solid), (ii) emission point position (1 m above roof level) (solid symbol, S1 blue/dark gray, S2 pale blue/light gray), (iii) control point position (1.5 m above ground) (empty symbol, P1 blue/dark gray, P2 pale blue/light gray).

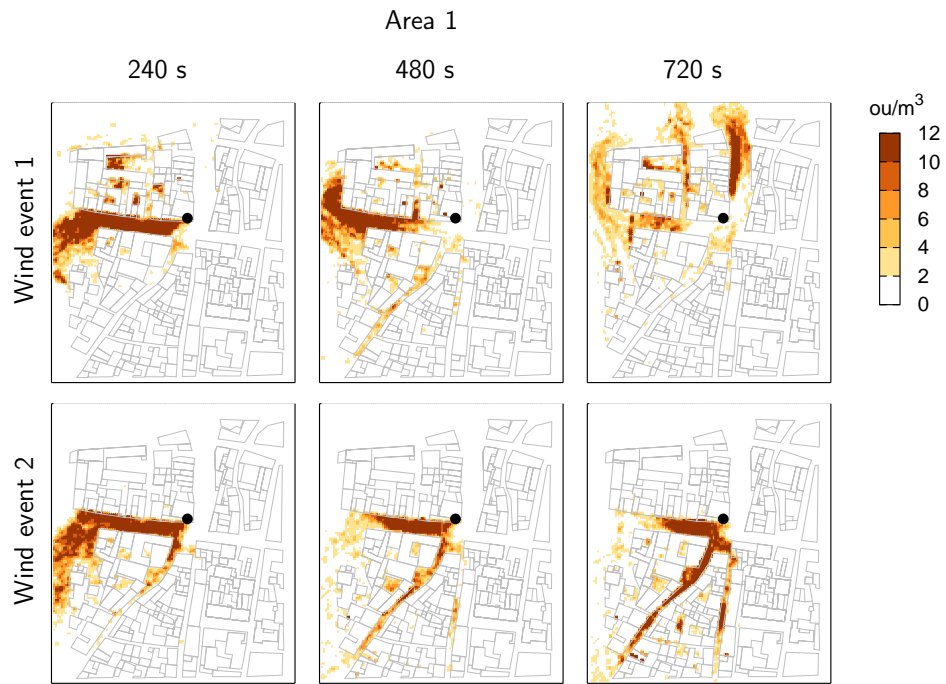


Figure 4: Isocontours of odor concentration calculated for Area 1 and wind event 1 and 2. Values are shown for a plane $z = 1.5 \text{ m}$ above the ground: snapshots are taken at every 240 s.

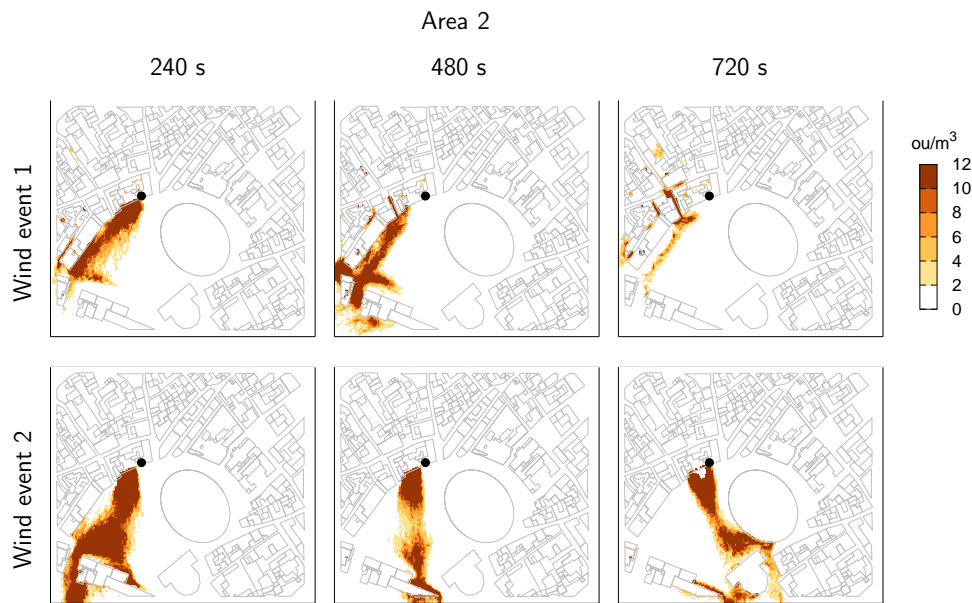


Figure 5: Isocontours of odor concentration calculated for Area 2 and wind event 1 and 2. Values are shown for a plane $z = 1.5 \text{ m}$ above the ground: snapshots are taken at every 240 s.

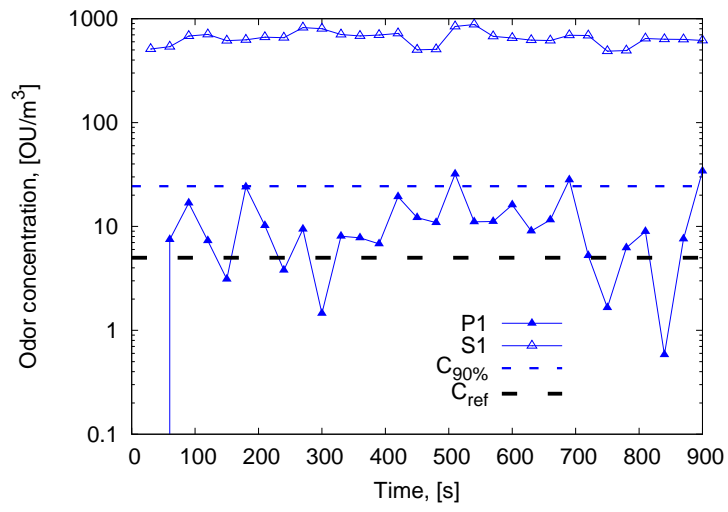


Figure 6: Time series of 30 seconds average odor concentration calculated at point P1 (closed symbol) and S1 (open symbol) for wind event 1: dashed lines represent 90th percentile of odor concentration for point P1 (thin dashed line) and a reference odor concentration threshold ($5 \text{ ou}/\text{m}^3$, thick dashed line) sufficient to cause nuisance.

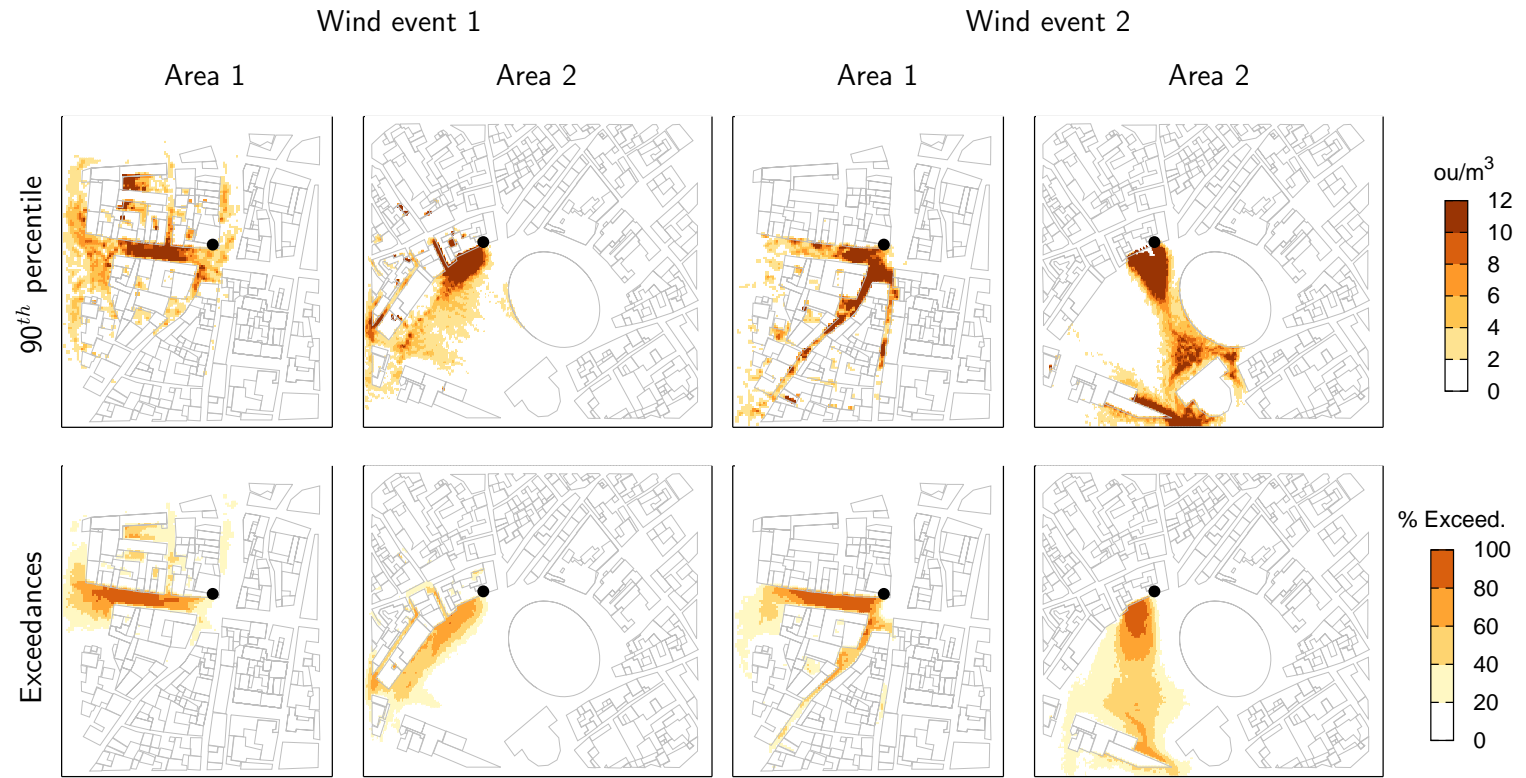


Figure 7: Statistics for odor impact assessment: (a) 90th percentile of odor concentration and (b) percent of exceedances ($C > 5 \text{ ou/m}^3$) during wind event 1 and 2 in Area 1 and 2.

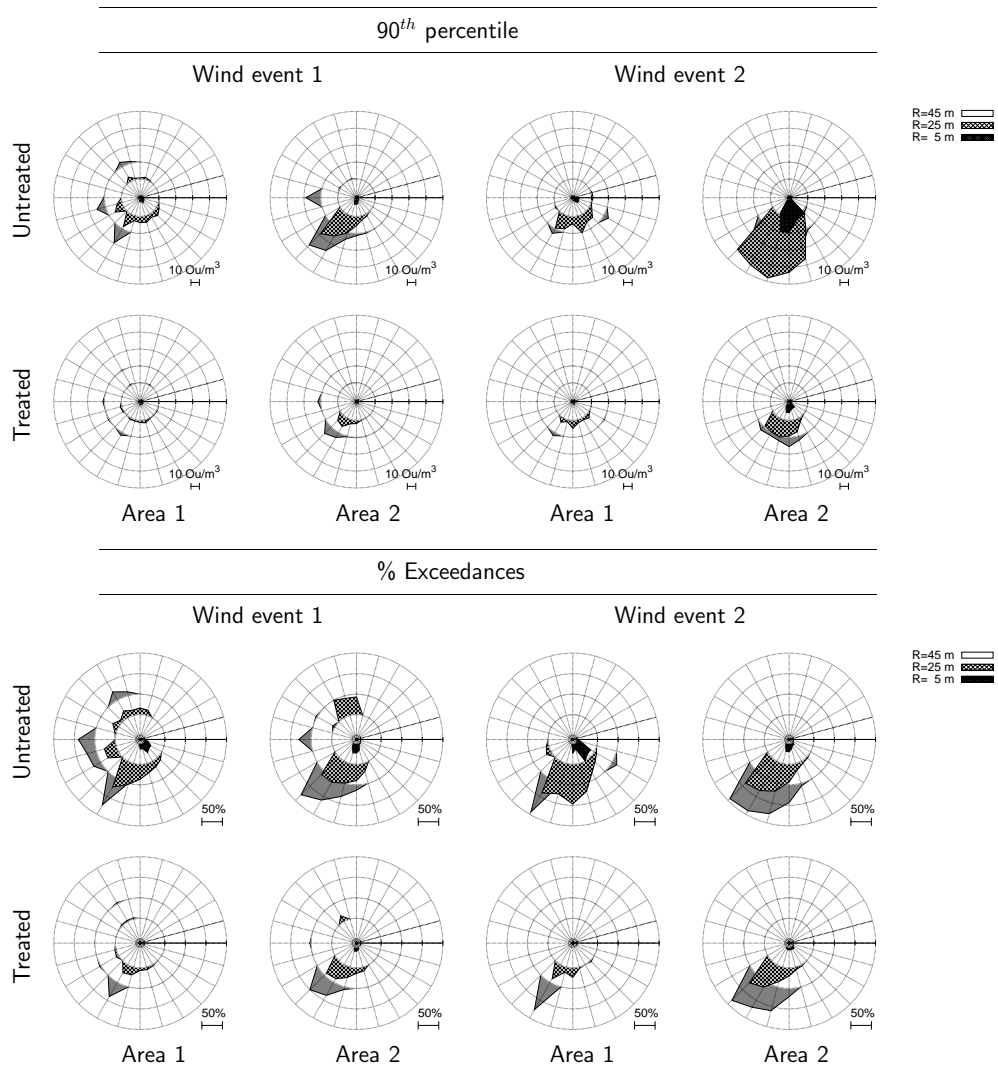


Figure 8: Odor rose of 90th percentile of odor concentration and % Exceedances for untreated and treated emission S1 and S2 and wind event 1 and 2.

Sample N.	$T, [^{\circ}C]$	RH, [%]	$Q, [Nm^3/s]$	$C, [ou/m^3]$
U-1	31.3	24.1	5.4	5,000
U-2	29.5	22.4	6.2	3,800
U-3	32.2	28.7	5.9	5,000
Average	31.0	25.07	5.83	4,600
T-1	30.8	24.6	6.0	1,300
T-2	30.3	22.7	4.3	1,300
T-3	30.9	23.5	4.5	2,000
Average	30.7	23.6	4.93	1,533

Table 1: Results of odor source sampling: U (untreated) identifies odor emission with abatement system turned off, T (treated) identifies odor emission with abatement system turned on.